Evaluation of thermal evaporation conditions used in coating aluminum on near-field fiber-optic probes

Christopher W. Hollars and Robert C. Dunn[a)]
Department of Chemistry, University of Kansas, Lawrence, Kansas 66045

(Received 8 January 1998; accepted for publication 9 January 1998)

The effects that the thermal evaporation conditions have on the roughness of aluminum-coated near-field fiber-optic probes were investigated using the high-resolution capabilities of atomic force microscopy. The coating conditions studied include the effects of background gas composition, base vacuum pressure, and aluminum evaporation rate. The effects of aging on the aluminum-coated tips were also evaluated. The results from topography measurements of the resulting aluminum film indicated that the most dramatic improvements in the tip coatings can be achieved using high aluminum evaporation rates at base vacuum pressures below 10^{-5} Torr. These results agree with other studies on thin aluminum films and reflect a decrease in oxide formation. For demanding applications of near-field microscopy requiring maximal resolution, the results presented here indicate that it may also be necessary to reduce oxygen and/or water from the vacuum chamber prior to coating. © *1998 American Institute of Physics.* [S0034-6748(98)01104-6]

I. INTRODUCTION

Near-field scanning optical microscopy (NSOM) is an emerging method that is rapidly taking its place among the many types of high-resolution scanning probe techniques.[1–3] The high spatial resolution and single molecule fluorescence detection limits of NSOM offer unique capabilities that are finding applications across the disciplines. Recent applications include studies on single molecules at room temperature,[4–7] aggregates,[8,9] quantum well devices,[10–12] and biological systems both dry and in aqueous environments.[13–16] The results from these studies have illustrated the unique information accessible with this optical technique.

In near-field scanning optical microscopy, high-resolution optical images are formed by scanning a subwavelength size spot of light in close proximity to a sample surface. The near-field probes used to deliver the light usually consist of a single-mode optical fiber that has been heated and pulled to a sharp point, approximately 50–100 nm in diameter.[1] In the taper region of the probe, where the waveguide properties of the fiber breakdown, 50–100 nm of aluminum are coated around the sides of the probe to confine the light so that it only exits the aperture at the very end of the tip. Aluminum is chosen because of its excellent reflectivity properties in the visible region of the spectrum, which reduces the amount of metal needed to confine the light. This is critical in near-field applications since the overall dimensions of the probe directly affect the ability to follow complicated sample topography, such as that encountered in biological applications. Unfortunately, aluminum is a challenging metal to evaporate free from contaminants, which can lead to rough films that have deleterious effects on near-field tip performance. Thus, for near-field microscopy, it is important to completely understand the aluminum-coating parameters, which lead to high-quality films for the specific geometry of the near-field probe.[17]

Numerous studies have reported on the propensity of aluminum to form oxides in the presence of both oxygen and water.[18–26] The oxide formation is generally accompanied by a decrease in film reflectivity and an increase in the film roughness, both of which can dramatically affect the performance of near-field probes.[27–30] For example, the reduction in reflectivity increases the amount of aluminum needed to confine the light within the near-field tip taper, which leads to an increase in the overall dimensions of the tip. An increase in film roughness will also compromise resolution by limiting the approach of the near-field tip to the sample surface. It is generally accepted that the NSOM tip must be positioned within one tip radius of the sample to attain the highest possible resolution.[31,32] For a near-field tip aperture of 50 nm, the tip must, therefore, be positioned within 25 nm of the sample surface. The formation of large oxide grains in the aluminum coating can restrict the ability to position the tip close to the sample surface, reducing the resolution in the near-field optical image.

The goal of this study is to explore the effects that various aluminum-coating conditions have on the final-coated near-field tip. The objective is to find the optimal parameters, which result in the smoothest possible aluminum coatings, thereby enhancing the imaging capabilities of near-field tips. To accomplish this, near-field tips were coated under a variety of conditions and the resulting aluminum films were evaluated using the high-resolution capabilities of atomic force microscopy (AFM).

II. EXPERIMENT

Near-field tips were fabricated from 125 μm single-mode optical fiber (3M) and pulled to a small tip approximately 100 nm in diameter using a modified Sutter P-2000

a)Author to whom correspondences should be addressed.

micropipette puller. The tapered optical fibers were coated with aluminum by thermal evaporation in a custom-built evaporation chamber. The chamber incorporates a stainless-steel base plate enclosed with a glass bell jar equipped with a viton seal. All components were connected to the chamber through conflat flanges in the base plate. The chamber is equipped with a Leybold Turbovac 151 turbopump and a Alcatel mechanical roughing pump. Chamber pressure is precisely monitored using a Bayard–Alpert type ion gauge and a thermocouple, both monitored with a Varian SenTorr gauge controller. Overnight pumping results in a base pressure of approximately 6×10^{-7} Torr.

For studies evaluating the participation of water in aluminum oxide formation, the chamber is baked from inside with a vacuum compatible quartz lamp heater (Kurt Lesker). The rate of application and thickness of the aluminum coating is monitored using a Leybold Inficon deposition monitor, fixed at a position of 5 cm above the near-field tips. The near-field tips are held in a custom-built assembly, which spins the tips continuously during the coating process, thereby exposing all sides of the tip taper to the aluminum source. The assembly contains adjustments to control the near-field tip angle, distance from the aluminum source, and tip rotation speed. Four near-field tips were coated simultaneously and for the studies reported here, the tips were fixed at an angle of 35° from the horizontal and rotated at a rate of approximately 5 Hz. For each coating run, approximately 5 in. of 1.0 mm diam aluminum wire (99.999%, Aldrich) was resistively melted in a fresh 1×5 cm tantalum boat cut from a 0.015 in. thick tantalum sheet. The chamber is equipped with a shutter placed between the tips and the aluminum source, which allows the aluminum to be melted and degassed before exposing the tips.

Immediately following coating the near-field tips, their optical quality was assessed qualitatively by visual inspection under 100× magnification with a compound microscope. Light from a HeNe laser (633 nm) was coupled into the near-field tips and they were examined for the quality of the spot emerging from the aperture and for the presence of pinholes. Tips that possessed pinholes or did not have a clearly defined spot emerging from the end were not used in this study. Exceptions to these criteria were made involving tips coated at elevated pressures.

For all the coating conditions studied, the thickness of the aluminum film deposited was held at a constant value experimentally determined to produce good near-field tips.[15,33] For the particular geometry of our evaporation chamber, a thickness of 5 kÅ as read on a thickness monitor positioned 5 cm above the near-field tips corresponds to a coverage of approximately 100 nm on the near-field tips, as determined from scanning electron microscopy (SEM) images. For comparative purposes, all tips studied were coated to a value of $5\ \text{kÅ}\pm10\%$. Near-field tips coated to a thickness outside of this range were rejected from the study since it has been shown previously that the roughness of the films increases with coating thickness.[29] Furthermore, with the exception of the rate study, all tips were coated at rates held as close as possible to 300 Å/s to provide for a controlled comparison. It is important to note that these numbers represent relative values, and are, therefore, only useful for comparative purposes to define trends in the coating characteristics.

The effects of age on the aluminum coating was investigated in light of results from previous studies that have shown a considerable evolution in the properties of aluminum coatings as a function of time.[27,28,34] Near-field tips stored under high oxygen atmospheres (30 atm) and normal atmospheric conditions showed no discernible structural changes in the aluminum coating over a 31 day period. Nevertheless, all NSOM tips used in this study were analyzed within 1 h of coating. Optical properties of the NSOM tips, such as output power or efficiency, were not used as part of the coating evaluation because of the sensitive dependence of these parameters on tip diameter.

The near-field tip aluminum coating roughness was evaluated by imaging the tips with an atomic force microscope from Digital Instruments (Nanoscope IIIa controller with a Dimension AFM) operating in contact mode. Standard silicon nitride tips with force constants of approximately 0.12 N/m were used in the imaging. The near-field tips were carefully mounted on their sides on microscope cover-slips using adhesives and imaged. Alignment of the near-field tips under the AFM tip was accomplished with the use of two 300× monocular scopes placed in an orthogonal arrangement. Using a micrometer to translate the near-field tip precisely under the AFM tip, the aluminum coating was imaged at two positions for each tip: 500 μm from the end of the tip (on the taper) and 1–1.2 mm from the end (just off the taper). Results from this and control studies, where images were collected progressively down the near-field tip taper, indicate no significant change in the aluminum properties as a function of position. Furthermore, at each position, a minimum of both a 5 μm×5 μm and a 2 μm×2 μm image were collected to guard against artifacts caused by local variations in the coating. Finally, because the near-field tips are shaped like tapered cylinders, steps were taken to avoid artifacts in the AFM images that may result from imaging off the apex of the near-field tip taper. Following the crude alignment of the AFM tip above the near-field tip using the 300× monoculars, the AFM tip was engaged onto the surface. The z piezodistance of the AFM tip was then monitored as the y piezo-offset was adjusted such that the AFM tip was moved to the highest point on the near-field taper region. This point corresponds to the apex of the near-field tip curvature and ensures that the same part of the AFM tips are used in the imaging. All images shown are unfiltered and were analyzed using Digital Instruments analysis software. Histograms of the aluminum surface topography were calculated with the bearing algorithm, which computes surface roughness based on deviations away from average height.

III. RESULTS

Although the aluminum coatings on NSOM tips are more difficult to analyze with AFM than coatings on flat substrates, actual NSOM tips were used in this study for several reasons. For one, the conical shape of the tip may play a role in the aluminum-coating properties that would

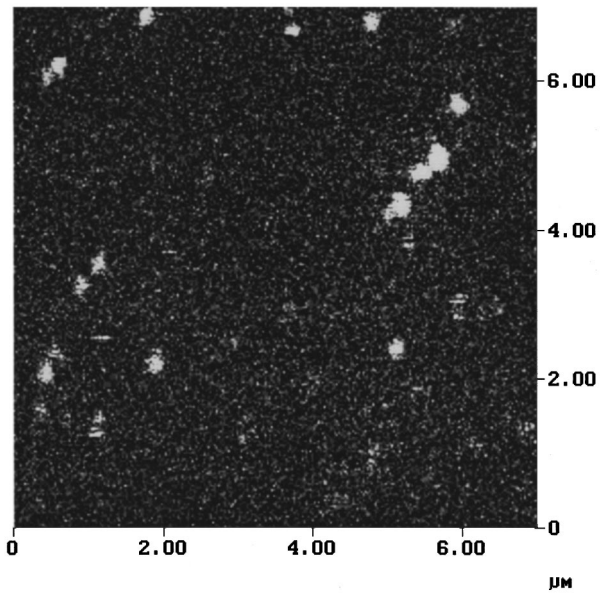

FIG. 1. 7 μm$\times$7 μm near-field fluorescence image of single sulforhodamine 101 molecules dispersed on a glass substrate. Each bright spot in the figure represents the fluorescence from a single dye molecule and has a FWHM of 90–100 nm, which reflects the aperture size of the particular near-field tip used to collect this image.

otherwise go undetected using flat substrates. Related to this concerns the fact that the tips are rotated during the coating process. This leads to a complicated coating process in which the tip sides are intermittently exposed to the aluminum source as they rotate. This would be impossible to mimic coating stationary flat substrates. We find that it is also very important to inspect the optical properties of the NSOM tips prior to analysis. This ensures that tips with macroscopic defects in the coating, such as pinholes, could be rejected from the study and kept from biasing the results. Pinholes in coated NSOM tips can usually be attributed to the presence of contaminants on the tip surface prior to coating and are not necessarily associated with problems in the aluminum film properties. Reducing the time between pulling the NSOM tip and loading it into the evaporation chamber along with keeping the chamber clean will usually eliminate any pinholes in the coating.

Before discussing the effects that coating parameters have on aluminum film quality, it is also important to demonstrate that the near-field tips under study are capable of subdiffraction-limit near-field fluorescence imaging. This capability is illustrated in Fig. 1, which shows a near-field fluorescence image of single sulforhodamine 101 molecules dispersed on a glass substrate. Each bright spot in Fig. 1 represents the fluorescence from a single molecule and has a full width at half maximum (FWHM) of approximately 100 nm, well beyond the classical diffraction limit. This size reflects the aperture diameter of the particular near-field tip used to collect this image and demonstrates the high spatial resolution and single molecule detection limits possible with these tips.

A. Vacuum background pressure

Given that oxide formation is known to degrade the reflectivity of aluminum, the most obvious parameter to investigate is that of background pressure in the evaporation chamber. It is well known that, in general, a reduction in vacuum pressure is accompanied by increases in aluminum film conductivity, density, and most importantly for near-field applications, a decrease in surface topography and increase in optical density.[28,34–36] The results from these studies, however, are difficult to extend to the particular case of near-field tips. While it is generally true that coatings improve with decreasing pressure, it is not a simple linear function. Reducing the background pressure in an evaporation chamber also becomes increasingly expensive and inconvenient. It is, therefore, important to know what vacuum base pressure is necessary to obtain the appropriate quality aluminum films for near-field microscopy.

To investigate these effects, the base vacuum in the coating chamber was changed over three orders of magnitude, ranging from 1×10^{-3} to 3×10^{-6} Torr. Not surprisingly, a decrease in the surface roughness of the aluminum film is observed in going to the lower pressures. Figure 2, panels A and B, show AFM images of NSOM tips coated at pressures of 1×10^{-3} and 3×10^{-6} Torr, respectively. Analysis of the AFM images results in the surface roughness histograms shown in the top panel of Fig. 3. Both a decrease in surface roughness and a narrowing in the distributions are observed in going from 10^{-3} to 10^{-6} Torr. The profiles in Fig. 3 are fit to a Gaussian function (solid line) and the resulting mean peak values and standard deviations are reported in the inset table. From this, it can be seen that at 10^{-3} Torr the NSOM tip coatings have a mean surface roughness of 68.1 nm with a distribution standard deviation of 24.9 nm. This is compared to tips coated under similar conditions but at a background pressure of 3×10^{-6} Torr. At this pressure, the mean surface roughness is significantly reduced to 16.1 nm and the distribution standard deviation is narrowed to 2.2 nm.

Previous high-resolution SEM images and NSOM force images, suggest that the aluminum coating forms a rimmed structure around the end of the NSOM tip aperture. This rim, combined with the grain structure in the aluminum film observed here, will limit the approach of the NSOM tip to the sample surface and, therefore, the optical resolution. The tip aperture, unfortunately, is difficult to probe directly with AFM. However, a best-case estimate for NSOM resolution can be obtained by disregarding the rim structure and considering only the topography of the aluminum film. For films coated at 3×10^{-6} Torr, the grain structure observed in the AFM images suggests that the closest the NSOM tip can be positioned to the sample surface is approximately 15–20 nm. Using the widely accepted criterion that the NSOM tip must be positioned within one aperture radius of the sample, this translates into a minimum useful NSOM tip diameter of approximately 30–40 nm. This, however, represents an optimistic estimate and lower resolution is likely.

To gain insight into the mechanisms of aluminum oxide formation and the effect of pressure, two relationships are useful. The first relationship can be used to approximate the mean-free path for the gas molecules in the vacuum chamber at ambient temperature as a function of pressure. This can be approximated by

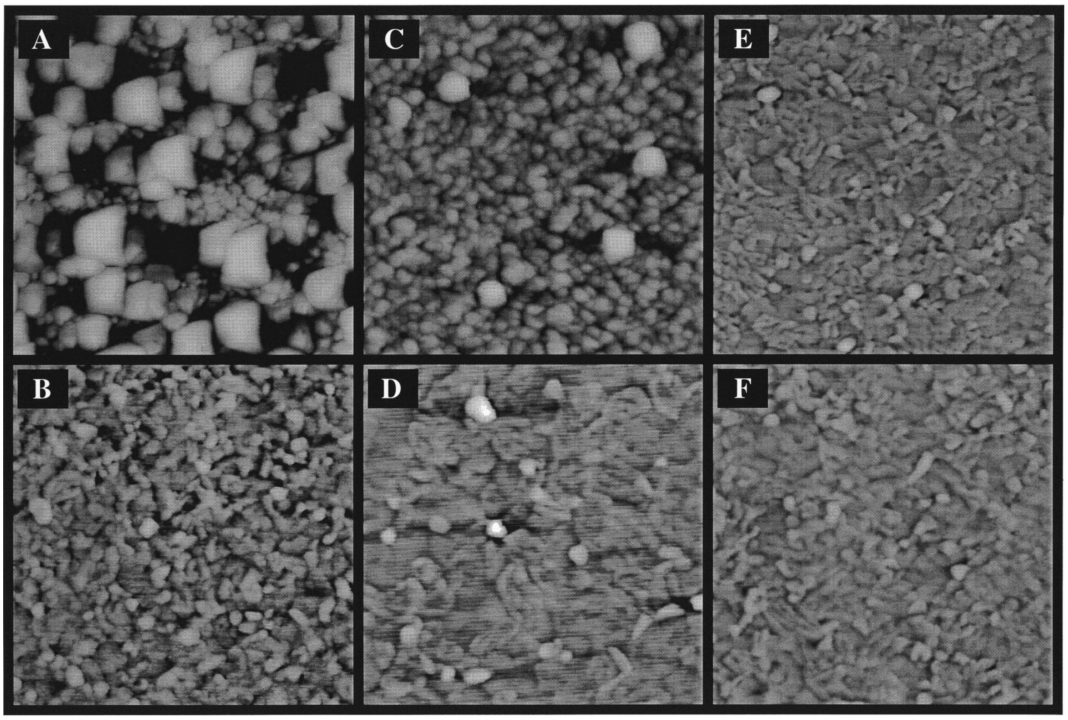

FIG. 2. Selected 2 μm$\times$2 μm AFM image of the aluminum coatings on near-field probes coated under the following conditions (A) 1.0×10^{-3} Torr, (B) 3.0×10^{-6} Torr, (C) 30 Å/s evaporation rate, (D) 2000 Å/s evaporation rate, (E) following oxygen gettering, and (F) after baking the chamber to decrease water. For the studies varying the chamber pressure (panels A and B) and under reduced oxygen and water (panels E and F) the evaporation rate was held at 300 Å/s. For all studies other than those varying the pressure, the vacuum was held constant at 1.0×10^{-5} Torr (panels C–F).

$$\lambda \approx 5\times10^{-3}/P, \tag{1}$$

where P is the vacuum pressure in Torr and λ is the mean-free path in centimeters.[37,38] Using this, the molecular mean-free path in vacuums below 10^{-4} Torr is greater than 50 cm, which is longer than the distance from the aluminum source to the near-field tips in our vacuum chamber (20 cm). This suggests that at pressures below 10^{-4} Torr, chemical reactions between the aluminum vapor and the background oxygen are unlikely to occur before the aluminum reaches the near-field tip surface. This leads to two possibilities—the aluminum reacts with oxygen during the coating process at the substrate surface and/or oxidation occurs rapidly upon breaking vacuum. While vacuum–ultraviolet studies suggest that the latter does occur to some extent,[27] evidence from these and other studies point to the former mechanism as the major source for oxide formation. Given this mechanism, it is instructive to consider the relative arrival rates between aluminum atoms and background gasses at the tip surface to further improve the coating quality.

The number of gas molecules impinging on a surface as a function of vacuum pressure can be approximated for ambient conditions by

$$N \approx 4\times10^{5}P, \tag{2}$$

where P is the pressure in Torr and N is given in monolayers (ML) per second.[37,38] Using this expression, the arrival rate of gas molecules at the near-field tip surface can be estimated. The calculated rates range from 400 ML/s at 10^{-3} Torr to 0.4 ML/s at 10^{-6} Torr. This can be compared to the aluminum arrival rate at the tip, which is estimated using evaporation rates calculated from coating times and SEM data on the coating thickness. Using these values, a rate of 300 Å/s as read on the thickness monitor corresponds to an actual coating rate of approximately 60 Å/s at the near-field tip. Using an aluminum monolayer thickness of 2.5 Å leads to a coating rate of approximately 24 ML/s. At high vacuum pressures, the rate of background gas arrival at the near-field tip surface is comparable with that of aluminum and reaction to form oxides increases in probability. As the pressure is lowered, the rate of aluminum arrival at the tip surface outpaces that of the residual gases in the chamber and higher-purity films are produced. Given the expense and inconvenience of obtaining vacuums significantly below 10^{-6} Torr, increasing the rate at which the aluminum is evaporated onto the tips provides a simple route to improving film quality.

B. Aluminum deposition rate

The rate at which aluminum is deposited onto a surface has been found to greatly influence the properties of the resulting film.[34,39–41] As mentioned earlier, this arises from a competition between attack by residual gases at the freshly coated aluminum surface and the deposition of another layer of aluminum. The most important species to consider are oxygen and water, which have reported sticking coefficients on fresh aluminum surfaces of 0.03–0.054[24,42,43] and 0.05–1,[23,25] respectively.

To quantify the effects of coating rate, near-field tips

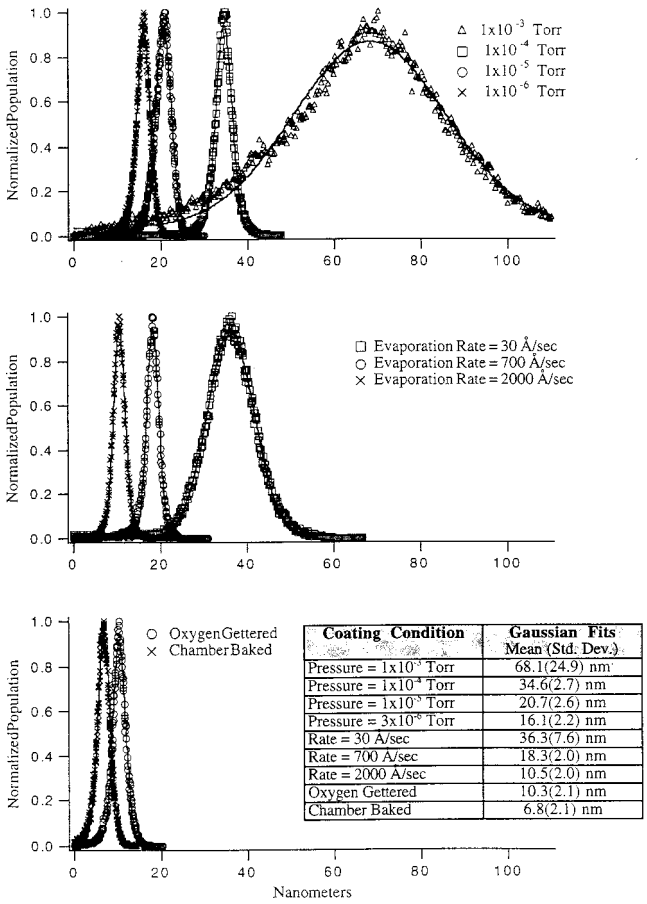

Coating Condition	Gaussian Fits Mean (Std. Dev.)
Pressure = 1x10⁻⁵ Torr	68.1(24.9) nm
Pressure = 1x10⁻⁴ Torr	34.6(2.7) nm
Pressure = 1x10⁻⁵ Torr	20.7(2.6) nm
Pressure = 3x10⁻⁶ Torr	16.1(2.2) nm
Rate = 30 A/sec	36.3(7.6) nm
Rate = 700 A/sec	18.3(2.0) nm
Rate = 2000 A/sec	10.5(2.0) nm
Oxygen Gettered	10.3(2.1) nm
Chamber Baked	6.8(2.1) nm

FIG. 3. Roughness histograms of the aluminum film topology measured by AFM (Fig. 2). The conditions varied include chamber base pressure (top panel), aluminum evaporation rate (middle panel), and background gas composition (bottom panel). Each distribution is fit with a Gaussian function (solid line) and the mean and standard deviation from these fits are reported in the inset table.

were coated at evaporation rates ranging from 30 to over 2000 Å/s. Figure 2, panels C and D, show AFM images of NSOM tips coated at 30 and 2000 Å/s, respectively. Roughness histograms calculated from AFM images of NSOM tips coated at rates of 30, 700, and 2000 Å/s, as read from the thickness monitor, are shown in Fig. 3 (middle panel). Adjusting these rates for the true rates at the tip, as done earlier, and converting this to aluminum coverage shows that these values correspond to coverage rates of approximately 3, 56, and 160 ML of aluminum per second. As a comparison, these studies were done at a vacuum base pressure of 1×10^{-5} Torr, where residual gas impinges on the near-field tip surface at a rate of approximately 4 ML/s. As the rate of evaporation is increased and the arrival of aluminum at the tip surface outpaces the arrival of background gasses, both a decrease in surface roughness and distribution are observed (inset table, Fig. 3). There is also a marked transition from the distinct grain structures observed at slower evaporation rates to a flowing-type structure observed at the highest deposition rate [see Figs. 2(C) and 2(D)].

C. Reduction of background oxygen and water

Active measures to control the background gas composition were investigated in an effort to reduce the partial pressures of oxygen and water. To actively reduce the partial pressure of oxygen in the chamber before coating, a 3 in.$\times$1 in. strip of tungsten was mounted in the chamber and resistively heated to getter oxygen. The well-known gettering effect of tungsten for oxygen at elevated temperatures and reduced pressures results from the facile formation of WO_3, which subsequently distills from the tungsten surface.[44,45] The decrease in oxygen partial pressure with time resulting from gettering at ambient temperatures follows the relation

$$\log P_{t=0} - \log P_t = 1.11\times10^4 \beta A t/2.303V, \tag{3}$$

where P is the pressure of oxygen at time t, A is the area of the filament, V is the volume of the vacuum chamber in cm^3, and β is the ''accommodation coefficient'' of oxygen at a given tungsten filament temperature.[38,45] Using this relation, tabulated β values, and the chamber volume and filament dimensions, the oxygen partial pressure in the chamber was calculated to be reduced 90% through gettering at 1300 K for approximately 13 min. However, due to the approximations in some parameter values and to ensure maximum reduction of the residual oxygen, the chamber was gettered for 2 h prior to coating the near-field tips.

In addition to oxygen, the presence of water during the coating process can lead to the undesirable formation of oxides.[22,23,25,46,47] Oxide formation through this pathway has been previously studied and shown to have a very complicated pressure dependence. However, while the grain structure shows complex behavior with respect to background water, the reflectivity of films at 550 nm steadily decreases with increasing presence of water.[25] To decrease the amount of water within the evaporation chamber, a quartz heating lamp was mounted inside the chamber and used to bake the chamber during pumping. The chamber was evacuated to a pressure of 1×10^{-5} Torr and baked with the quartz lamp for a time of 8 h. The lamp was then turned off and the chamber was allowed to cool under vacuum for an additional 8 h to insure that the near-field tips were at room temperature before coating.

Both of these methods resulted in improved aluminum coatings. Figure 2, panels E and F, show AFM images of NSOM tips coated following oxygen gettering and baking of the chamber, respectively. Figure 3 (bottom panel) plots the surface roughness histograms and shows that both films exhibit smaller grain sizes than those observed in the pressure and rate studies. Baking the chamber results in a significant reduction in the mean roughness of the films over the best coatings observed at low pressures or high evaporation rates. Oxygen gettering also resulted in a reduction in the film grain size, although not as dramatic as that observed following baking. For demanding applications of NSOM requiring the highest spatial resolution, the gains provided by both baking and gettering the chamber may prove to be essential. For less demanding applications, however, the gain in film quality is probably not sufficient to warrant the added inconvenience and time required to bake the chamber. Gettering, however, is a fast and relatively easy way to improve the aluminum film quality.

IV. DISCUSSION

The results presented here illustrate the effects that various coating parameters have on obtaining high-quality aluminum coatings for use in fabricating near-field fiber-optic probes. While not exhaustive, the parameters explored provide guidance in coating near-field tips suitable for most applications. It should also be mentioned that during the course of these studies, several attempts were made to cool the near-field tips with liquid nitrogen during the coating process. It has been previously shown that cooling the substrate can substantially reduce the topography of the evaporated aluminum film by limiting the diffusion distance of the aluminum atoms on the substrate surface.[29,38] Unfortunately, we observed little improvement in the roughness of the film compared to tips coated at ambient temperatures, which likely reflects the difficulty in cooling near-field tips. While cooling will probably remain problematic, an alternative scheme that reduces the radiant heating of the tips during the coating process, such as electron-beam evaporation techniques, may provide an attractive direction for the future.

The optical quality of the aluminum film evaporated onto near-field probes is becoming an increasingly important issue as the resolution in near-field microscopy is pushed towards its theoretical limit. Given that the throughput of light through a near-field aperture goes as r^6, where r is the tip radius,[32] the need for highly reflective aluminum coatings becomes critical to minimize light leakage from the taper region and maximize tip efficiency. The need to position the near-field probe near the sample surface to obtain the highest possible resolution also places constraints on the aluminum-coating topography. Again, as the theoretical resolution limit is approached the ability to position the tip within an aperture radius of the sample becomes problematic and requires extremely smooth aluminum coatings. The findings presented here illustrate the need to coat near-field tips under vacuum pressures below 10^{-5} Torr and at the highest possible aluminum evaporation rates. For demanding applications, reducing the background of water and oxygen will also improve the coating quality and will likely become more important as the resolution in near-field microscopy is increased.

ACKNOWLEDGMENTS

The authors R.C.D. and C.W.H. would like to thank M. Annie Lee for the careful reading of the manuscript. We gratefully acknowledge the support of NSF (CHE-9612730), NSF-CAREER (CHE-9703009), and the University of Kansas.

[1] E. Betzig, J. K. Trautman, T. D. Harris, J. S. Weiner, and R. L. Kostelak, Science **251**, 1468 (1991).
[2] E. Betzig and J. K. Trautman, Science **257**, 189 (1992).
[3] D. W. Pohl, in *Advances in Optical and Electron Microscopy*, edited by T. Mulvey and C. J. R. Sheppard (Academic, London, 1991), Vol. 12, pp. 243–312.
[4] X. S. Xie and R. C. Dunn, Science **265**, 361 (1994).
[5] J. K. Trautman, J. J. Macklin, L. E. Brus, and E. Betzig, Nature **369**, 40 (1994).
[6] W. P. Ambrose, P. M. Goodwin, J. C. Martin, and R. A. Keller, Science **265**, 364 (1994).
[7] E. Betzig and R. J. Chichester, Science **262**, 1422 (1993).
[8] D. A. Higgins and P. F. Barbara, J. Phys. Chem. **99**, 3 (1995).
[9] S. K. Kook and R. Kopelman, J. Phys. Chem. **96**, 10 672 (1992).
[10] H. F. Hess, E. Betzig, T. D. Harris, L. N. Pfeiffer, and K. W. West, Science **264**, 1740 (1994).
[11] S. K. Buratto, J. W. P. Hsu, J. K. Trautman, E. Betzig, R. B. Bylsma, C. C. Bahr, and M. J. Cardillo, J. Appl. Phys. **76**, 7720 (1994).
[12] R. D. Grober, T. D. Harris, J. K. Trautman, E. Betzig, W. Wegscheider, L. Pfeiffer, and K. West, Appl. Phys. Lett. **64**, 1421 (1994).
[13] R. C. Dunn, G. H. Holtom, L. Mets, and X. S. Xie, J. Phys. Chem. **98**, 3094 (1994).
[14] E. Betzig, R. J. Chichester, F. Lanni, and D. L. Taylor, Bioimaging **1**, 129 (1993).
[15] C. E. Talley, G. Cooksey, and R. C. Dunn, Appl. Phys. Lett. **69**, 3809 (1996).
[16] H. Muramatsu, N. Chiba, K. Homma, K. Nakajima, T. Ataka, S. Ohta, A. Kusumi, and M. Fujihira, Appl. Phys. Lett. **66**, 3245 (1995).
[17] G. A. Valaskovic, M. Holton, and G. H. Morrison, Appl. Opt. **34**, 1215 (1995).
[18] P. B. Barna, F. M. Reicha, G. Barcza, L. Gosztola, and F. Koltai, Vacuum **33**, 25 (1983).
[19] N. K. Sandle and H. Wilman, J. Phys. D: Appl. Phys. **6**, 1025 (1973).
[20] C. W. B. Martinson and S. A. Flodstrom, Surf. Sci. **80**, 306 (1979).
[21] C. W. B. Martinson, S. A. Flodstrom, J. Rundgren, and P. Westrin, Surf. Sci. **89**, 102 (1979).
[22] W. Eberhardt and C. Kunz, Surf. Sci. **75**, 719 (1978).
[23] W. H. Krueger and S. R. Pollack, Surf. Sci. **30**, 280 (1972).
[24] W. H. Krueger and S. R. Pollack, Surf. Sci. **30**, 263 (1972).
[25] M. J. Verkerk and W. A. M. C. Brankaert, Thin Solid Films **139**, 77 (1986).
[26] A. Barna, P. B. Barna, G. Radnoczi, F. M. Reicha, and L. Toth, Phys. Status Solidi A **55**, 427 (1979).
[27] R. P. Madden, L. R. Canfield, and G. Hass, J. Opt. Soc. Am. **53**, 620 (1963).
[28] G. Hass, W. R. Hunter, and R. Tousey, J. Opt. Soc. Am. **47**, 1070 (1957).
[29] J. E. Curran, J. S. Page, and U. Pick, Thin Solid Films **97**, 259 (1982).
[30] J. H. Halford and F. K. Chin, J. Opt. Soc. Am. **63**, 786 (1973).
[31] H. A. Bethe, Phys. Rev. **66**, 163 (1944).
[32] C. J. Bouwkamp, Philips Res. Rep. **5**, 401 (1950).
[33] C. W. Hollars and R. C. Dunn, J. Phys. Chem. **101**, 6313 (1997).
[34] G. Hass, W. R. Hunter, and R. Tousey, J. Opt. Soc. Am. **46**, 1009 (1956).
[35] G. Hass, J. Opt. Soc. Am. **45**, 945 (1955).
[36] R. W. Fane and W. E. J. Neal, J. Opt. Soc. Am. **60**, 790 (1970).
[37] J. R. Black, Natl. Bur. Stand. Spec. Pub. **337**, 398 (1970).
[38] S. Dushman, *Scientific Foundations of Vacuum Technique* (Wiley, New York, 1962).
[39] G. Hass and J. E. Waylonis, J. Opt. Soc. Am. **51**, 719 (1961).
[40] N. G. Dhere and T. P. Arsenio, Thin Solid Films **30**, 267 (1975).
[41] P. Glaser and E. Szigeti, Vacuum **33**, 31 (1983).
[42] G. Dorey, Surf. Sci. **27**, 311 (1971).
[43] D. N. Popov, T. K. Kotlarova, T. D. Uzunov, and V. N. Gaydarova, Vacuum **38**, 1015 (1988).
[44] I. Langmuir, J. Am. Chem. Soc. **35**, 105 (1913).
[45] I. Langmuir, J. Am. Chem. Soc. **37**, 417 (1915).
[46] R. W. Springer and D. S. Catlett, J. Vac. Sci. Technol. **15**, 210 (1978).
[47] J. D. Reimer, J. Vac. Sci. Technol. A **2**, 242 (1984).